

Novel Sandwiched Intermetallic Selenoantimonates: Soft Synthesis and Characterization of $\text{Cu}_2\text{SbSe}_3 \cdot 0.5\text{en}$ and $\text{Cu}_2\text{SbSe}_3 \cdot \text{en}^\dagger$

Zhen Chen, Ryan E. Dilks, Ru-Ji Wang, Jack Y. Lu, and Jing Li*

Department of Chemistry, Rutgers University, Camden, New Jersey 08102

Received April 2, 1998. Revised Manuscript Received June 16, 1998

Two novel two-dimensional (layered) intermetallic copper selenoantimonates $\text{Cu}_2\text{SbSe}_3 \cdot 0.5\text{en}$ (**I**) and $\text{Cu}_2\text{SbSe}_3 \cdot \text{en}$ (**II**), have been prepared by soft solvothermal reactions of CuCl , SbCl_3 , and Se with A_2Se ($\text{A} = \text{Na}, \text{K}$) in the presence of ethylenediamine. Single-crystal X-ray diffraction analyses show that both structures crystallize in the monoclinic crystal system. Compound **I** belongs to the $P2_1/n$ (no. 14) space group with $a = 6.399(1) \text{ \AA}$, $b = 18.858(4) \text{ \AA}$, $c = 6.786(1) \text{ \AA}$, $\beta = 113.23(3)^\circ$, $Z = 4$, $V = 752.5(2) \text{ \AA}^3$, and **II** belongs to the Pn (no. 7) space group with $a = 6.321(2) \text{ \AA}$, $b = 11.841(2) \text{ \AA}$, $c = 6.932(2) \text{ \AA}$, $\beta = 111.59(2)^\circ$, $Z = 2$, $V = 482.4(2) \text{ \AA}^3$. Both compounds consist of Cu_2SbSe_3 layers separated by free ethylenediamine molecules. The intermetallic layers are very similar in **I** and **II**, but the orientations of the solvent molecules are different. Both compounds contain copper atoms of mixed-valence, Cu(I) and Cu(II) , and both are semiconductors with intermediate band gaps ($\sim 1.6 \text{ eV}$).

Introduction

Hundreds of solid-state intermetallic sulfuroantimonates have been reported. Comparably, intermetallic selenoantimonates have not been extensively investigated. The limited examples include ASbSe_2 ($\text{A} = \text{Na}, \text{K}, \text{Cs}$),^{1–3} A_3SbSe_4 ($\text{A} = \text{Na}, \text{K}, \text{Rb}, \text{Cs}$),^{4,5} RbSb_3Se_5 ,⁶ $\text{Ba}_4\text{Sb}_4\text{Se}_{11}$,⁷ $\text{Tl}_l\text{Sb}_m\text{Se}_n$ ($l = 1–3$; $m = 1–2$, $n = 2–4$),^{8–11} and MSb_2Se_4 ($\text{M} = \text{Ba}, \text{Sn}, \text{Pb}$).^{12–14} The only known copper-based selenoantimonates are CuSbSe_2 ,¹⁵ Cu_3SbSe_3 ,¹⁶ and Cu_3SbSe_4 .¹⁷ CuSbSe_2 has a layer structure and both Cu_3SbSe_3 and Cu_3SbSe_4 are composed of three-dimensional frameworks. All three were prepared by

solid-state direct synthesis at relatively high temperatures.

Use of supercritical ethylenediamine (en ; $300–350^\circ\text{C}$) in the synthesis of metal chalcogenides is known.¹⁸ Recently, we have focused on a softer route in which mild solvothermal conditions are applied to reactions in en medium at temperatures generally $<180^\circ\text{C}$. Under such conditions, both the solubility and the diffusion rate of the solid species are significantly increased compared with the ambient temperature and pressure, and the crystallization process is greatly enhanced. This synthetic route is especially promising for the synthesis of metal polychalcogenides because the very mild solution medium stabilizes the polychalcogen building blocks and allows Q_y^{2-} ($y \geq 2$) ions to incorporate and remain intact in the final structure. This leads to the formation of a wide variety of new compounds that exhibit a diverse and rich structural chemistry, most of which are metastable and are not accessible by high-temperature methods. The mild conditions also allow en , the organic solvent, to act as a reactive reagent by chelating a metal center to form a complex cation in the resultant compound. Some examples include $[\text{M}(\text{en})_3]_2(\text{Hg}_2\text{Te}_6)$ ¹⁹ ($\text{M} = \text{Fe}, \text{Mn}$), $\{\text{Mn}(\text{en})_3\}_2\text{Cl}_2\}\text{Hg}_2\text{Te}_4$,¹⁹ $[\text{M}(\text{en})_3]_2\text{Sn}_2\text{Q}_6$ ($\text{M} = \text{Mn}, \text{Zn}$, $\text{Q} = \text{Se}, \text{Te}$)²⁰ $[\text{Fe}$

[†] In memory of Professor Jean Rouxel.

* To whom correspondence should be addressed.

(1) Kuznetsov, V. G.; Kanishcheva, A. S.; Salov, A. V. *Zhurnal Neorganicheskoi Khim.* **1974**, *19*, 1280.

(2) Dittmar, G.; Schaefer, H. *Acta Crystallogr. B* **1992**, *48*, 113.

(3) Kanishcheva, A. S.; Mikhailov, Yu. B. S.; Lazarev, V. Bu. B.; Moshchalkova, N. A. *Doklady Akademii Nauk SSSR* **1980**, *252*, 872.

(4) Eisenmann, B.; Zagler R. Z. *Naturforsch(B)* **1989**, *44*, 249.

(5) Sheldrick, W. S.; Wachhold, M. Z. *Naturforsch(B)* **1996**, *51*, 32.

(6) Sheldrick, W. S.; Heaesler, H. J. *Z. Anorg. Allg. Chem.* **1988**, *557*, 98.

(7) Cox, D. E.; Moodenbaugh, A. R.; Sleight, A. W.; Chen, H. Y. *National Bureau of Standards (U. S.), Special Publication* **1980**, *567*, 189.

(8) Wacker, K.; Salk, M.; Decker-Schultheiss, G.; Keller, E. *Z. Anorg. Allg. Chem.* **1991**, *606*, 51.

(9) Olsen, A.; Goodman, P.; Whitfield, H. J. *J. Solid State Chem.* **1985**, *60*, 305.

(10) Pinsker, Z. G.; Hitrovkha, V. I. *Kristallografiya* **1956**, *1*, 300.

(11) Pinsker, Z. G.; Semiletov, S. A.; Belova, E. N. *Doklady Akademii Nauk SSSR* **1956**, *106*, 1003.

(12) Cordier, G.; Schaefer, H. Z. *Naturforsch(B)* **1979**, *34*, 1053.

(13) Smith, P. K.; Parise, J. B. *Acta Crystallogr. B* **1985**, *41*, 84.

(14) Skowron, A.; Boswell, F. W.; Corbett, J. M.; Taylor, N. J. *J. Solid State Chem.* **1994**, *112*, 251.

(15) Imamov, R. M.; Pinsker, Z. G.; Ivchenko, A. I. *Kristallografiya* **1964**, *9*, 853.

(16) Pfitzner, A. *Z. Anorg. Allg. Chem.* **1995**, *621*, 685.

(17) Pfitzner, A. *Z. Kristallografiya* **1994**, *209*, 685.

(18) Wood, P. T.; Pennington, W. T.; Kolis, J. W. *J. Am. Chem. Soc.* **1992**, *114*, 9233. Wood, P. T.; Pennington, W. T.; Kolis, J. W. *J. Chem. Soc., Chem. Commun.* **1993**, 235. Wood, P. T.; Pennington, W. T.; Kolis, J. W. *Inorg. Chem.* **1994**, *33*, 1556. Jerome, J. E.; Wood, P. T.; Pennington, W. T.; Kolis, J. W. *Inorg. Chem.* **1994**, *33*, 1733.

(19) Li, J.; Rafferty, B. G.; Mulley, S.; Proserpio, D. M. *Inorg. Chem.* **1995**, *34*, 6417. Li, J.; Chen, Z.; Kelley, J. L.; Proserpio, D. M. In *Solid State Chemistry of Inorganic Materials*, ISBN: 1–55899–357–6, **1997**; Vol. 453, pp 29–34.

(20) Whittingham, T. K.; Chen, Z.; Li, J.; Proserpio, D. M. *Bull. N. J. Acad. Sci.* **1998**, *42*, 11.

(en)₃[enH]SbSe₄,²² [La(en)₄Cl]In₂Te₄,²³ [M(en)₃]In₂Te₆ (M = Fe, Zn),²⁴ and [Mo₃(en)₃(Te₂)₃(O)(Te)]In₂Te₆,²⁴ all recently synthesized by us. The metal complexes in these compounds are in general large in size and they actively affect the geometric construction and reorganization of the Q_y²⁻ building blocks. The resultant structures are typically zero- (molecular) or one-dimensional (chainlike). The only known examples of two-dimensional (layered) structures containing en-metal complexes are [Ga(en)₃]In₃Te₇²⁵ and [Co(en)₃]-CoSb₄S₈,²⁶ where the metal complex cations are sandwiched between the anionic layers. In other cases when alkali metals are actively involved in the reactions, en may function solely as a solvent, as in the syntheses of Rb₂Hg₃Te₄,²⁷ Rb₂Hg₆Se₇,²⁸ RbHgSbTe₃,²⁹ AHgSbSe₃,³⁰ (A = K, Rb, Cs), Cs₂PdSe₈,³¹ and RbAg₅Se₃.³² Here we report the solvothermal synthesis and characterization of two novel layered intermetallic copper selenoantimonates, Cu₂SbSe₃·0.5en (**I**) and Cu₂SbSe₃·en (**II**), whose structures are different from the two groups just discussed in that the solvent (en) incorporates into the framework structures as free molecules.

Experimental Section

Materials. CuCl (99.9%), SbCl₃(99+%), and Se (99.5%) powder were purchased from Strem Company. Na₂Se and K₂Se were prepared by reactions of alkali metal and elemental selenium in a 2:1 ratio in liquid ammonia. Ethylenediamine (99%, anhydrous, Fisher Scientific) was used as a solvent in all reactions.

Crystal Growth. Single crystals of **I** and **II** were grown from solvothermal reactions containing 0.059 g of Se, 0.025 g of CuCl, 0.057 g of SbCl₃, 0.031 g of Na₂Se (**I**), and 0.039 g of K₂Se (**II**). The starting materials were weighed and mixed in a glovebox under argon atmosphere. The samples were then transferred to thick-walled Pyrex tubes, and ~0.4 mL of solvent (en) was added to each sample. After the liquid was condensed by liquid nitrogen, the tubes were sealed with a torch under vacuum (~10⁻³ Torr). The samples were then heated at 160 °C for 7 days. After being cooled to room temperature, the mixtures were washed with water and ethanol and then dried with anhydrous diethyl ether. Quantitative amounts of orange, column-like crystals of **I** (>95% yield) were isolated from the first sample and orange, platelike crystals of **II** (~95% yield) were obtained from the second sample. The approximate compositions of **I** and **II** were established from microprobe analysis on a JEOL JXA-8600 Superprobe.

Crystal Structure Determination. An orange column-shaped crystal of **I** (0.2 × 0.3 × 0.4 mm) and an orange platelike crystal of **II** (0.05 × 0.2 × 0.3 mm) were selected for the crystal structure analysis. Each crystal was mounted on

Table 1. Crystallographic Data for Cu₂SbSe₃·0.5en(I) and Cu₂SbSe₃·en(II)

parameter	I	II
formula	Cu ₂ SbSe ₃ ·0.5en	Cu ₂ SbSe ₃ ·en
formula weight	515.76	545.81
crystal system	monoclinic	monoclinic
space group	<i>P</i> 2 ₁ / <i>n</i> (No.14)	<i>Pn</i> (No.7)
<i>a</i> , Å	6.399(1)	6.321(2)
<i>b</i> , Å	18.858(4)	11.841(2)
<i>c</i> , Å	6.786(1)	6.932(2)
β, deg	113.23(3)	111.59(2)
<i>V</i> , Å ³	752.5(2)	482.4(2)
<i>d</i> _{calc} , g/cm ³	4.553	3.757
<i>Z</i>	4	2
λ, Å	0.71073	0.71073
μ(Mo Kα), mm ⁻¹	23.572	18.397
<i>T</i> , °C	21	21
unique reflections	1315	914
observed [<i>I</i> > 2σ (<i>I</i>)]	1191	905
GOF ^a on <i>F</i> _o ²	1.626	1.352
<i>R</i> indices [<i>I</i> > 2σ (<i>I</i>)]	<i>R</i> 1 ^b 0.0382, <i>wR</i> 2 ^c 0.0726	<i>R</i> 1 0.0276, <i>wR</i> 2 0.0581
<i>R</i> indices (all data)	<i>R</i> 1 0.0426, <i>wR</i> 2 0.0730	<i>R</i> 1 0.0279, <i>wR</i> 2 0.0581

^a GOF = [Σw(*F*_o² - *F*_c²)/(*n* - *p*)]^{1/2}, where *n* is the number of reflections and *p* is the number of refined parameters. ^b *R*1 = Σ||*F*_o|| - ||*F*_c||/Σ||*F*_o||. ^c *wR*2 = [Σ(*F*_o² - *F*_c²)/Σw*F*_o⁴]^{1/2}; weighting: *w* = {1 - exp[-2 × sin²(θ/λ)]}/σ²(*F*_o²) for **I**; *w* = {1 - exp[-sin²(θ/λ)]}/σ²(*F*_o²) for **II**.

a glass fiber in air on an Enraf-Nonius CAD4 automated diffractometer, and 25 reflections were centered in each case using graphite-monochromated Mo Kα radiation. Least-squares refinement of their setting angles resulted in the unit cell parameters reported in Table 1, together with other details associated with data collection and refinement. Data were collected with ω-scan method within the limits 6 ≤ 2θ ≤ 50°. An empirical absorption correction based on Ψ-scans was applied to all data. Both structures were solved by direct methods and refined by full-matrix least-squares on *F*_o². Ethylenediamine molecules in compound **I** showed an orientational disorder, and the disordered C(1) atoms were labeled as C(1) and C(1A). In the final refinement, their site occupancy factors were assigned to be 0.7 and 0.3, respectively. No such a disorder was observed for **II**. Anisotropic thermal displacements were assigned to all non-hydrogen atoms. All calculations were performed using SHELX-97.³³ Crystal structure drawings were produced with SCHAKAL.³⁴ Final atomic coordinates and average temperature factors are listed in Table 2, and selected bond lengths and angles for **I** and **II** are reported in Tables 3 and 4, respectively.

Thermal Analysis. Thermogravimetric (TGA) analyses of the title compounds were performed on a computer-controlled TA Instrument 2050TGA analyzer. Powder samples of **I** (11.8660 mg) and **II** (10.2540 mg) were loaded into alumina pans and heated with a ramp rate of 10 °C/min from room temperature to 400 °C. The samples were examined by powder X-ray diffraction immediately after the TGA experiments.

Diffuse Reflectance Measurements. To estimate the band gaps of the title compounds, a Shimadzu UV-3101PC double-beam, double-monochromator spectrophotometer was used to perform optical diffuse reflectance measurements of **I** and **II**. Data were collected in the wavelength range 250–1800 nm. BaSO₄ powder was used as a standard (100% reflectance). A similar procedure as previously described²⁹ was used to collect and convert the data using the Kubelka–Munk function.³⁵ The scattering coefficient (*S*) was treated as a

(21) Chen, Z.; Li, J.; Emge, T. J.; Yuen, T.; Proserpio, D. M. *Inorg. Chim. Acta* **1998**, *273*, 310.

(22) Girard, M. R.; Li, J.; Proserpio, D. M. *Main Group Metal Chem.* **1998**, *21*, 231.

(23) Li, J.; Chen, Z.; Chen, F.; Proserpio, D. M. *Inorg. Chim. Acta* **1998**, *273*, 255.

(24) Li, J.; Chen, Z.; Emge, T. J.; Proserpio, D. M. *Inorg. Chem.* **1997**, *36*, 1437.

(25) Li, J.; Chen, Z.; Proserpio, D. M., manuscript in preparation.

(26) Stephan, H.-O.; Kanatzidis, M. G. *J. Am. Chem. Soc.* **1996**, *118*, 122–126.

(27) Li, J.; Chen, Z.; Lam, K.-C.; Mulley, S.; Proserpio, D. M. *Inorg. Chem.* **1997**, *36*, 684.

(28) Lam, K.-C.; Li, J., unpublished results.

(29) Li, J.; Chen, Z.; Wang, X.-X.; Proserpio, D. M. *J. Alloys Comput.* **1997**, *262–263*, 28–33.

(30) Chen, Z.; Wang, R.-J.; Li, J., manuscript in preparation.

(31) Li, J.; Chen, Z.; Wang, R.-J.; Lu, J. *J. Solid State Chem.*, in press.

(32) Chen, Z.; Wang, R.-J.; Li, J., manuscript in preparation.

(33) Sheldrick, G. M. *SHELX-97: program for structure refinement*; University of Goettingen: Germany, 1997.

(34) Keller, E. *SCHAKAL 92: a computer program for the graphical representation of crystallographic models*; University of Freiburg: Germany, 1992.

(35) Wendlandt, W. W.M.; Hecht, H. G. *Reflectance Spectroscopy*; Interscience: A Division of John Wiley & Sons: New York, 1966.

Table 2. Atomic Coordinates and Equivalent Isotropic Displacement Parameters (Å²) for I and II

compound atom	I				II			
	<i>x</i>	<i>y</i>	<i>z</i>	<i>U</i> _{eq} ^a	<i>x</i>	<i>y</i>	<i>z</i>	<i>U</i> _{eq} ^a
Sb(1)	0.1530(1)	0.69745(4)	0.0694(1)	0.0163(2)	0.8847(1)	0.58329(8)	0.4617(1)	0.0129(2)
Cu(1)	0.0492(2)	0.82601(8)	0.1698(2)	0.0266(4)	0.9917(3)	0.3795(2)	0.3656(3)	0.0217(4)
Cu(2)	0.1054(3)	0.67969(8)	-0.4106(3)	0.0341(4)	0.9335(4)	0.6079(2)	0.9416(3)	0.0298(5)
Se(1)	0.5332(2)	0.69746(6)	0.0212(2)	0.0194(3)	1.1185(2)	0.7175(1)	0.7523(2)	0.0154(3)
Se(2)	-0.0857(2)	0.61240(6)	-0.2276(2)	0.0198(3)	0.5068(2)	0.5870(1)	0.5193(2)	0.0164(3)
Se(3)	0.2589(2)	0.60943(6)	0.3846(2)	0.0186(3)	0.7807(2)	0.7212(1)	0.1507(2)	0.0149(3)
N(1)	-0.219(2)	0.0400(6)	0.252(2)	0.035(2)	0.326(2)	0.829(1)	0.252(2)	0.025(3)
N(2)					0.089(2)	1.126(1)	0.170(2)	0.028(3)
C(1) ^b	-0.020(4)	-0.004(1)	0.380(1)	0.034(4)	0.265(3)	0.945(2)	0.153(3)	0.032(4)
C(2)					0.141(3)	1.013(1)	0.263(3)	0.024(3)
C(1A)	0.132(1)	-0.003(2)	0.540(6)	0.024(8)				

^a *U*_{eq}, defined as one-third of the trace of the orthogonalized **U** tensor. ^b The site occupancy factors of C(1) and C(1A) in **I** were assigned to be 0.7 and 0.3, respectively.

Table 3. Selected Bond Lengths (Å) and Angles (deg) for Cu₂SbSe₃·0.5en (I)^a

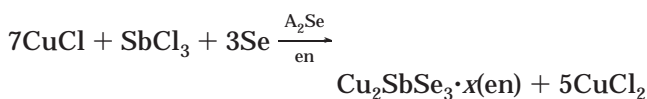
Sb(1)–Se(1)	2.580(1)	Se(2)–Cu(2)	2.418(2)
Sb(1)–Se(2)	2.557(1)	Se(3)–Cu(1b)	2.417(2)
Sb(1)–Se(3)	2.578(1)	Se(3)–Cu(2d)	2.393(2)
Sb(1)–Cu(1)	2.672(2)	Cu(2)–Cu(1a)	2.674(2)
Sb(1)–Cu(2)	3.168(2)	N(1)–C(1)	1.48(2)
Se(1)–Cu(1a)	2.467(2)	C(1)–C(1e)	1.56(1)
Se(1)–Cu(2b)	2.372(2)	N(1)–C(1Ae)	1.47(4)
Se(2)–Cu(1c)	2.452(2)	C(1A)–C(1Ae)	1.56(1)
Se(1)–Sb(1)–Se(2)	101.52(4)	Sb(1)–Cu(1)–Se(3c)	116.29(6)
Se(1)–Sb(1)–Se(3)	98.78(5)	Sb(1)–Cu(1)–Cu(2f)	105.20(6)
Se(1)–Sb(1)–Cu(1)	111.97(5)	Se(1f)–Cu(1)–Se(2b)	102.04(7)
Se(1)–Sb(1)–Cu(2)	65.32(5)	Se(1f)–Cu(1)–Se(3c)	123.53(7)
Se(2)–Sb(1)–Se(3)	97.47(5)	Se(1f)–Cu(1)–Cu(2f)	75.19(6)
Se(2)–Sb(1)–Cu(1)	129.71(5)	Se(2b)–Cu(1)–Se(3c)	109.52(7)
Se(2)–Sb(1)–Cu(2)	48.53(4)	Se(2b)–Cu(1)–Cu(2f)	153.31(8)
Se(3)–Sb(1)–Cu(1)	112.53(5)	Se(3c)–Cu(1)–Cu(2f)	55.81(5)
Se(3)–Sb(1)–Cu(2)	132.26(5)	Sb(1)–Cu(2)–Se(1c)	91.70(6)
Cu(1)–Sb(1)–Cu(2)	115.16(5)	Sb(1)–Cu(2)–Se(2)	52.43(4)
Sb(1)–Se(1)–Cu(1a)	121.56(6)	Sb(1)–Cu(2)–Se(3 g)	139.50(7)
Sb(1)–Se(1)–Cu(2b)	95.51(5)	Sb(1)–Cu(2)–Cu(1a)	97.52(7)
Cu(1a)–Se(1)–Cu(2b)	106.52(7)	Se(1c)–Cu(2)–Se(2)	120.93(7)
Sb(1)–Se(2)–Cu(1c)	97.61(6)	Se(1c)–Cu(2)–Se(3 g)	121.38(7)
Sb(1)–Se(2)–Cu(2)	79.04(6)	Se(1c)–Cu(2)–Cu(1a)	100.87(7)
Cu(1c)–Se(2)–Cu(2)	102.92(7)	Se(2)–Cu(2)–Se(3 g)	114.44(8)
Sb(1)–Se(3)–Cu(1b)	101.97(6)	Se(2)–Cu(2)–Cu(1a)	125.82(8)
Sb(1)–Se(3)–Cu(2d)	95.24(6)	Se(3 g)–Cu(2)–Cu(1a)	56.65(5)
Cu(1b)–Se(3)–Cu(2d)	67.55(6)	N(1)–C(1)–C(1e)	108(2)
Sb(1)–Cu(1)–Se(1f)	101.13(6)	N(1e)–C(1A)–C(1Ae)	108(3)
Sb(1)–Cu(1)–Se(2b)	101.39(6)		

^a Symmetry transformations: *a* (0.5 + *x*, 1.5 – *y*, –0.5 + *z*); *b* (0.5 + *x*, 1.5 – *y*, 0.5 + *z*); *c* (–0.5 + *x*, 1.5 – *y*, –0.5 + *z*); *d* (*x*, *y*, 1 + *z*); *e* (–*x*, –*y*, 1 – *z*); *f* (–0.5 + *x*, 1.5 – *y*, 0.5 + *z*); *g* (*x*, *y*, –1 + *z*).

constant because it has been shown to be independent of wavelength for particles sufficiently large (>5 μm). The average particle size used in our measurements is significantly larger (>20 μm).

Results and Discussion

Synthesis. The solvothermal reactions of CuCl, SbCl₃, and Se with A₂Se (A = Na, K) in the presence of en yielded Cu₂SbSe₃·0.5en (**I**) and Cu₂SbSe₃·en (**II**) according to the following overall equation:



where, *x* = 0.5 for **I**, *x* = 1 for **II**, and A = Na, K. The reactions involved a redox process in which oxidation of Cu⁺ to Cu²⁺ and reduction of Se to Se²⁻ occurred. Although the alkali metal did not appear in the final products, the high yield of the reactions just presented

Table 4. Selected Bond Lengths (Å) and Angles (deg) for Cu₂SbSe₃·en (II)^a

Sb(1)–Cu(1)	2.656(2)	Cu(1)–Se(3c)	2.451(2)
Sb(1)–Se(1)	2.564(2)	Cu(2)–Se(1)	2.429(3)
Sb(1)–Se(2)	2.564(2)	Cu(2)–Se(2c)	2.375(3)
Sb(1)–Se(3)	2.589(2)	Cu(2)–Se(3d)	2.423(3)
Cu(1)–Cu(2a)	2.649(3)	N(1)–C(1)	1.51(2)
Cu(1)–Se(1b)	2.477(2)	N(2)–C(2)	1.48(2)
Cu(1)–Se(2a)	2.470(2)	C(1)–C(2)	1.52(2)
Cu(1)–Sb(1)–Se(1)	129.32(6)	Cu(1e)–Cu(2)–Se(2c)	101.73(10)
Cu(1)–Sb(1)–Se(2)	113.09(7)	Cu(1e)–Cu(2)–Se(3d)	57.59(7)
Cu(1)–Sb(1)–Se(3)	112.00(6)	Se(1)–Cu(2)–Se(2c)	123.30(10)
Se(1)–Sb(1)–Se(2)	99.65(6)	Se(1)–Cu(2)–Se(3d)	113.85(10)
Se(1)–Sb(1)–Se(3)	99.19(6)	Se(2c)–Cu(2)–Se(3d)	119.33(10)
Se(2)–Sb(1)–Se(3)	98.81(6)	Sb(1)–Se(1)–Cu(2)	80.83(8)
Sb(1)–Cu(1)–Cu(2a)	104.22(8)	Sb(1)–Se(1)–Cu(1c)	99.69(7)
Sb(1)–Cu(1)–Se(1b)	101.53(7)	Cu(2)–Se(1)–Cu(1c)	99.94(9)
Sb(1)–Cu(1)–Se(2a)	101.65(8)	Sb(1)–Se(2)–Cu(2b)	93.62(8)
Sb(1)–Cu(1)–Se(3c)	115.01(8)	Sb(1)–Se(2)–Cu(1e)	121.72(7)
Cu(2a)–Cu(1)–Se(1b)	154.25(11)	Cu(1e)–Se(2)–Cu(2b)	107.63(9)
Cu(2a)–Cu(1)–Se(2a)	76.65(8)	Sb(1)–Se(3)–Cu(1b)	104.48(8)
Cu(2a)–Cu(1)–Se(3c)	56.56(7)	Sb(1)–Se(3)–Cu(2f)	96.52(8)
Se(1b)–Cu(1)–Se(2a)	98.00(7)	Cu(1b)–Se(3)–Cu(2f)	65.85(8)
Se(1b)–Cu(1)–Se(3c)	111.75(9)	N(1)–C(1)–C(2)	110.1(14)
Se(2a)–Cu(1)–Se(3c)	125.32(9)	N(2)–C(2)–C(1)	109.6(14)
Cu(1e)–Cu(2)–Se(1)	122.96(10)		

^a Symmetry transformations: *a* (0.5 + *x*, 1 – *y*, 0.5 – *z*); *b* (0.5 – *x*, 1 – *y*, 0.5 – *z*); *c* (0.5 + *x*, 1 – *y*, 0.5 + *z*); *d* (*x*, *y*, 1 + *z*) *e* (0.5 – *x*, 1 – *y*, 0.5 + *z*); *f* (*x*, *y*, –1 + *z*).

involving use of monoselenides (Na₂Se and K₂Se) makes it apparent that they played a role in the formation of the title compounds. Subsequent reactions using only CuCl, SbCl₃, and Se in en gave a mixture of **I** and **II** (with a very low yield of **II**) along with a polycrystalline impurity phase (>50%) that cannot be identified by powder X-ray diffraction analysis.

Structures. Depicted in Figure 1 are two perspective views of **I** (Figure 1a) and **II** (Figure 1b). Both compounds are composed of two-dimensional intermetallic Cu₂SbSe₃ layers separated by free en molecules. The Cu₂SbSe₃ layers are very similar in the two structures. The center of each layer coincides with the crystallographic *n*-glide plane at *y* = 0.25 and 0.75 for **I** and *y* = 0.5 for **II**. The antimony atom Sb(1) has a distorted tetrahedral coordination with Cu(1) and three selenium atoms, Se(1), Se(2), and Se(3) (see Figure 2). The average Sb–Se distance, 2.572 Å for both **I** and **II**, is comparable with those reported for the three known copper selenoantimonate compounds. The Sb(1)–Cu(1) bond lengths, 2.672 Å in **I** and 2.656 Å in **II**, are considerably shorter than those found in the known phases. The distances between Sb(1) and Cu(2) are 3.168(2) and 3.239(2) Å in **I** and **II**, respectively. A

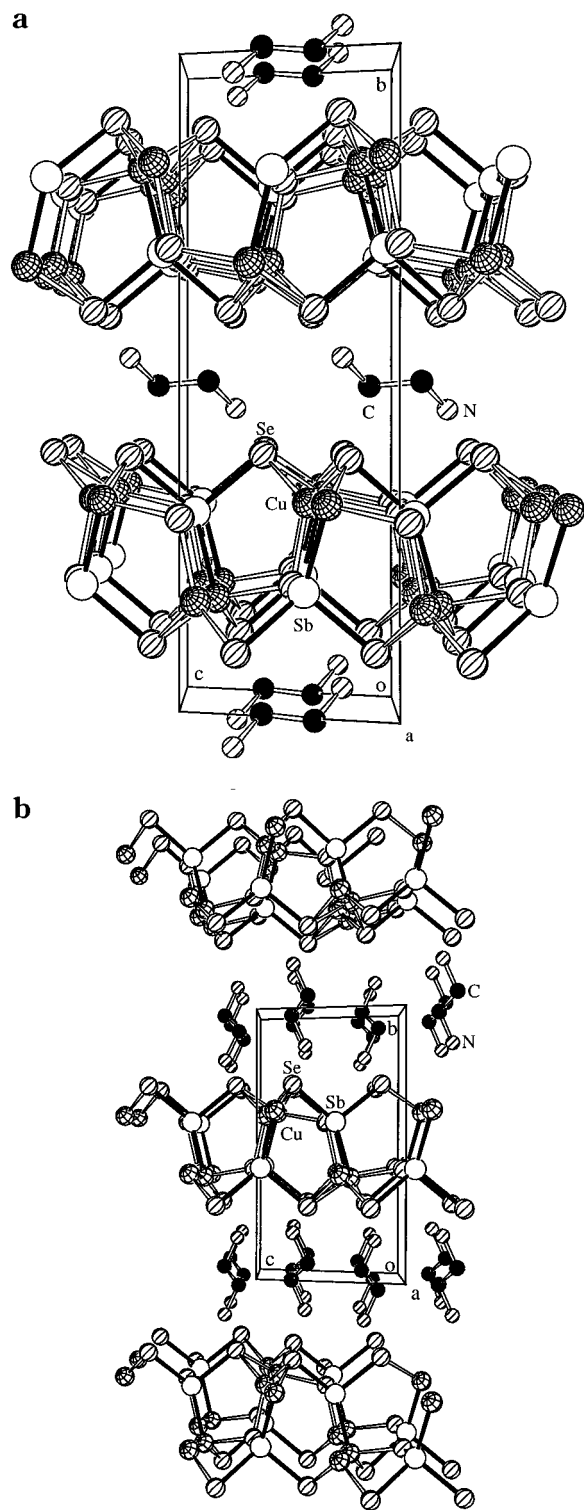


Figure 1. Perspective views along *a* direction. (a) $\text{Cu}_2\text{SbSe}_3 \cdot 0.5\text{en}$ (**I**); (b) $\text{Cu}_2\text{SbSe}_3 \cdot \text{en}$ (**II**). Large open circles are Sb atoms, large shaded circles are Se, and cross shaded circles are Cu atoms. Carbon atoms are represented by small solid circles and nitrogen atoms by small shaded circles.

similar Sb–Cu contact of 3.165(3) Å is observed in Cu_3SbSe_3 . Both Cu(1) and Cu(2) coordinate to three Se atoms in a trigonal [Cu(1)] and nearly trigonal planar [Cu(2)] configuration. The average Cu(1)–Se and Cu(2)–Se distances are 2.445(2), 2.394(2) Å in **I** and 2.466(2), 2.409(3) Å in **II**, respectively. These results are again comparable with those observed in the three known compounds. There is also a short contact

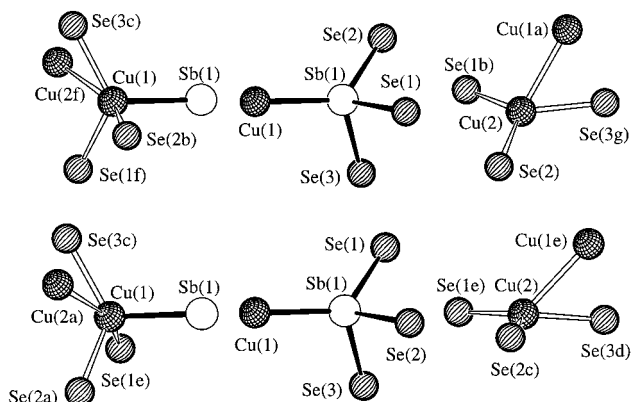


Figure 2. Coordination geometry for Cu(1), Sb, and Cu(2). Top: $\text{Cu}_2\text{SbSe}_3 \cdot 0.5\text{en}$ (**I**); bottom: $\text{Cu}_2\text{SbSe}_3 \cdot \text{en}$ (**II**).

between Cu(1) and Cu(2) (2.674(2) Å in **I** and 2.649(3) Å in **II**) compared with the Cu(1)–Cu(2) distances of 2.665 Å in Cu_3SbSe_3 and 2.830 Å in Cu_3SbSe_4 . Formal oxidation state assignment suggests mixed valences for the two coppers, Cu(I) and Cu(II), assuming a +3 for Sb and a –2 for Se.³⁶ Each selenium is bonded to one Sb atom and two Cu atoms [Cu(1) and Cu(2)] to give a trigonal coordination. No short Se–Se contacts are found in the two structures, which is consistent with the oxidation state assignment just presented. The free en molecules are situated between the Cu_2SbSe_3 layers to give rise to a sandwich structure. The C–C bonds in en molecules are approximately parallel to the Cu_2SbSe_3 layers in **I**, and are approximately perpendicular to the Cu_2SbSe_3 layers in **II**, as illustrated in Figure 1. The interlayer distances are ~5 Å (**I**) and 6.8 Å (**II**), and the shortest intermolecular distances between the en nitrogen atom and the selenium of the Cu_2SbSe_3 layer are 3.339 Å (**I**) and 3.407 Å (**II**).

A close look at the three known copper selenoantimonates reveals some structural differences between these and the title compounds. Cu_3SbSe_3 ¹⁶ and Cu_3SbSe_4 ,¹⁷ for example, contain three-dimensional networks. The copper atoms in both structures have tetrahedral coordination with selenium atoms, in contrast with the trigonal coordination of Cu to Se in the title compounds. The coordination of Sb atoms is also quite different in Cu_3SbSe_3 and Cu_3SbSe_4 . CuSbSe_2 ¹⁵ possesses a two-dimensional layer structure as in **I** and **II**. However, the coordination of Cu in this compound is again tetrahedral to Se, in comparison with the trigonal coordination of Cu to Se in the title compounds. The Sb has a three coordination to Se, however, no short Cu–Cu and Sb–Cu bonds are observed in this structure, as found in both **I** and **II**. Another unique feature that distinguishes the title compounds from all three known copper selenoantimonates is the incorporation of free en molecules between the inorganic layers. The very different orientations of the same species in the two compounds suggest that the inorganic layers are highly mobile and flexible. They may be active in certain ion-exchange and intercalation reactions.

Thermal Analysis. Figure 3 shows the data of thermogravimetric analysis performed on **I** (solid line)

(36) Arrangements are being made for electron spin resonance and magnetic susceptibility measurements to confirm the oxidation states of the copper atoms.

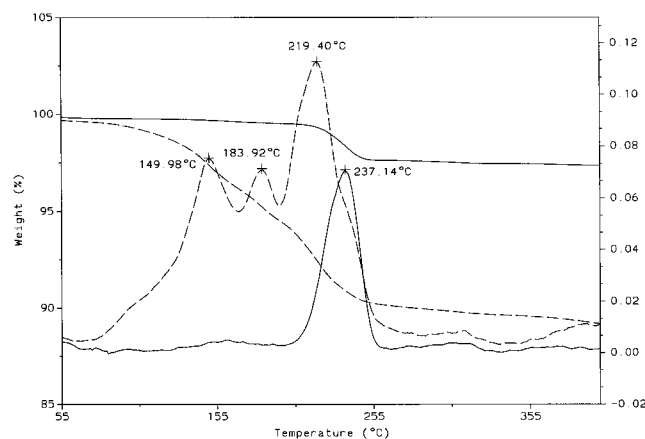


Figure 3. Thermogravimetric analysis (TGA) data showing weight losses of $\text{Cu}_2\text{SbSe}_3 \cdot 0.5\text{en}$ (**I**) (solid line) and $\text{Cu}_2\text{SbSe}_3 \cdot \text{en}$ (**II**) (dash line) between 55 and 400 °C. The negatives of the first derivatives ($\%/^\circ\text{C}$) are also plotted as a function of temperature.

and **II** (dash line). The weight losses observed for both compounds, along with the first derivative curves ($\%/^\circ\text{C}$) are plotted as functions of temperature between 55 and 400 °C. These curves show that the weight loss of en in **I** is most likely a single-step process (peak temperature for the 1st derivative, 237 °C), whereas it is a three-step process for compound **II** (peak temperatures for the 1st derivative, 150, 184, and 219 °C). The difference in the decomposition temperatures of **I** and **II** can be attributed to the relative orientation and stability of the en molecules in the two compounds. Powder X-ray analysis performed immediately after the TGA experiments indicated the existence of Cu_3SbSe_4 and CuSe_2 in the residues of the samples.

Diffuse Reflectance Measurements. The optical properties of **I** and **II** were assessed by obtaining the optical diffuse reflectance data of these compounds. Figure 4 plots the Kubelka–Munk (or remission, F) function for both **I** and **II** converted from the diffuse reflectance data ($F = (1 - R_\infty)^2 / 2R_\infty$, where R_∞ is the relative diffuse reflectance of an infinitely thick layer. For practical purposes, this can be achieved at a layer

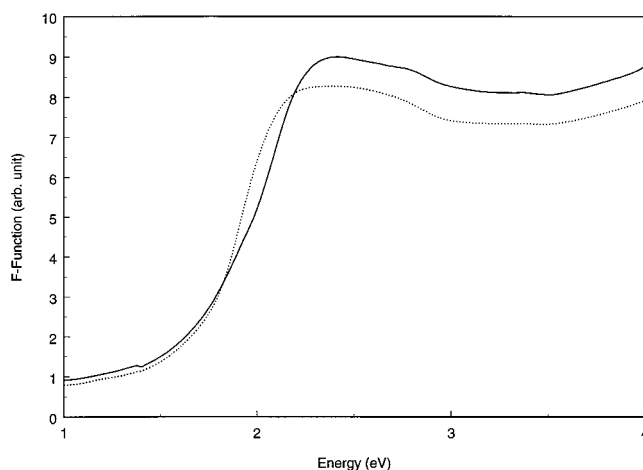


Figure 4. Optical absorption spectra (Kubelka–Munk function) for $\text{Cu}_2\text{SbSe}_3 \cdot 0.5\text{en}$ (**I**) (dotted line) and $\text{Cu}_2\text{SbSe}_3 \cdot \text{en}$ (**II**) (solid line).

depth of a few millimeters). The absorption coefficient (α) can be computed from the remission function ($F = \alpha/S$) where S is the scattering factor.^{29,35} From the sharp absorption edges the band gaps can be estimated and a values of 1.58 eV for **I** and 1.61 eV for **II** were obtained. This result confirms the semiconducting nature of both compounds.

Acknowledgment. Financial support from the National Science Foundation (Grant DMR-9553066) is greatly appreciated. We are also grateful to the Research Corporation for a Partners in Science participation for R.E.D. The FT-IR/TGA/DSC apparatus was purchased through a NSF ARI grant (CHE 9601710-ARI). We thank Andrea Knox for her help with the FT-IR/TGA/DSC instrument.

Supporting Information Available: Tables of atomic coordinates of all atoms, anisotropic thermal parameters, bond distances and angles, and crystallographic data for **I** and **II** (15 pages). Ordering information is given on any current masthead page.

CM980238A